



## Primordial Black Holes and $r$ -Process Nucleosynthesis

George M. Fuller,<sup>1,\*</sup> Alexander Kusenko,<sup>2,3,†</sup> and Volodymyr Takhistov<sup>2,‡</sup>

<sup>1</sup>*Department of Physics, University of California, San Diego, La Jolla, California 92093-0424, USA*

<sup>2</sup>*Department of Physics and Astronomy, University of California, Los Angeles, Los Angeles, California 90095-1547, USA*

<sup>3</sup>*Kavli Institute for the Physics and Mathematics of the Universe (WPI), UTIAS, University of Tokyo, Kashiwa, Chiba 277-8583, Japan*

(Received 6 April 2017; revised manuscript received 11 June 2017; published 7 August 2017)

We show that some or all of the inventory of  $r$ -process nucleosynthesis can be produced in interactions of primordial black holes (PBHs) with neutron stars (NSs) if PBHs with masses  $10^{-14} M_{\odot} < M_{\text{PBH}} < 10^{-8} M_{\odot}$  make up a few percent or more of dark matter. A PBH captured by a NS sinks to the center of the NS and consumes it from the inside. When this occurs in a rotating millisecond-period NS, the resulting spin-up ejects  $\sim 0.1 M_{\odot}$ – $0.5 M_{\odot}$  of relatively cold neutron-rich material. This ejection process and the accompanying decompression and decay of nuclear matter can produce electromagnetic transients, such as a kilonova-type afterglow and fast radio bursts. These transients are not accompanied by significant gravitational radiation or neutrinos, allowing such events to be differentiated from compact object mergers occurring within the distance sensitivity limits of gravitational-wave observatories. The PBH-NS destruction scenario is consistent with pulsar and NS statistics, the dark-matter content, and spatial distributions in the Galaxy and ultrafaint dwarfs, as well as with the  $r$ -process content and evolution histories in these sites. Ejected matter is heated by beta decay, which leads to emission of positrons in an amount consistent with the observed 511-keV line from the Galactic center.

DOI: 10.1103/PhysRevLett.119.061101

Primordial black holes (PBHs) can account for all or part of dark matter (DM) [1–13]. If a PBH is captured by a neutron star (NS), it settles into the center and grows until the supply of nuclear matter is exhausted by accretion and ejection.

In this Letter we show that NS disruptions by PBHs in DM-rich environments, such as the Galactic center (GC) and dwarf spheroidal galaxies, provide a viable site for  $r$ -process nucleosynthesis, thus offering a solution to a long-standing puzzle [14–18]. The transients accompanying NS disruption events and the positrons produced in these events are consistent with present observations, and they offer a way of testing the NS-PBH scenario in the future.

We will demonstrate that, when a PBH accretes matter inside a rapidly rotating millisecond pulsar (MSP), the resulting pulsar spin-up causes  $\sim 0.1 M_{\odot}$ – $0.5 M_{\odot}$  of neutron-rich material to be ejected without significant heating and only modest neutrino emission. This provides a favorable setting for  $r$ -process nucleosynthesis, occurring on the Galactic time scales, which can evade several problems that have challenged the leading proposed  $r$ -process production sites, such as neutrino-heated winds from core-collapse supernovae or binary compact object mergers (COMs) [19,20]. The unusual distribution of  $r$ -process abundances within the ultrafaint dwarf spheroidal galaxies (UFDs) [21,22] is naturally explained by the rates of PBH capture in these systems. The rates are also consistent with the paucity of pulsars in the GC [23]. A similar distribution of  $r$ -process material in UFDs can be expected from NS disruptions due to black holes produced in the NS interiors

by accretion of particle dark matter onto the NS [24], although the rates and the implications for dark-matter properties are, of course, different. The probability of PBH capture depends on both the PBH and the NS densities. DM-rich environments, such as the GC and dwarf spheroidal galaxies, are not known to host NSs. An exception is the young magnetar [25,26], whose age is small compared to the time scales of PBH capture. NSs are found in the disk and the halo, as well as in the globular clusters, where the dark-matter density [27,28] is too low to cause a substantial decrease in the pulsar population. Positrons emitted from the heated neutron-rich ejecta can account for the observed 511-keV line from the GC [29,30]. The final stages of neutron-star demise can be the origin [31,32] of some of the recently observed [33] fast radio bursts (FRBs), as well as x-ray and  $\gamma$ -ray transients. A kilonova-type [34–41] afterglow can accompany the decompressing nuclear matter ejecta, but unlike COMs, these events are not associated with a significant release of neutrinos or gravitational radiation. Therefore, future observations of gravitational waves and kilonovae will be able to distinguish between  $r$ -process scenarios.

Millisecond pulsars are responsible for the predominant contribution to the nucleosynthesis initiated by PBH-induced centrifugal ejection of neutron-rich material, since MSPs have the highest angular velocities at the time of PBH capture. The most prominent sites of  $r$ -process production must have a high density of MSPs as well as PBHs. The latter trace the DM spatial distribution. The DM density is high in the GC and in the UFDs. On the other

hand, the MSP density is high in molecular clouds, including the central molecular zone (CMZ), and the globular clusters. While the CMZ is located within the GC with an extremely high DM density, observations imply that the DM content of globular clusters is fairly low [27,28]. The product of the DM density and the MSP density is still sufficient to allow for some  $r$ -process nucleosynthesis in both the UFDs and the globular clusters, but we estimate that CMZ accounts for 10% to 50% of the total Galactic production. We include contributions from the GC (CMZ) and the rest of the halo (which may be comparable, within uncertainties) [42,43].

The CMZ has an approximate size of  $\sim 200$  pc and is located near the GC, where supernova rates are the highest. Since the DM density peaks at the GC, the CMZ is a site of frequent PBH-MSP interactions. The pulsar formation rate [44] in the CMZ is  $1.5 \times 10^{-3} \text{ yr}^{-1}$  (7% of the Galactic formation rate), consistent with the GeV  $\gamma$ -ray flux observed [45] from the GC by the Fermi Large Area Telescope. Hence, we expect  $N_p^{\text{GC}} \approx 1.5 \times 10^7$  NSs to be produced at the GC during the lifetime of the Galaxy,  $t_G \sim 10^{10}$  yr. Roughly 30%–50% of these NSs become MSPs [46], and the number of MSPs with a particular rotation period can then be estimated from a population model [46–48].

Simulations and observations of UFDs imply [21] that  $\sim 2000$  core-collapse supernovae have occurred in 10 UFDs during  $t_{\text{UFD}} \sim 5 \times 10^8$  yr. Hence, we expect that  $N_p^{\text{UFD}} \sim 10^2$  pulsars have been produced in each of these systems, on average, and we estimate the fraction of fast-rotating MSPs using a population model [47].

The black-hole capture rate can be calculated using the initial PBH mass ( $m_{\text{PBH}}$ ), DM density and velocity dispersion (assuming a Maxwellian distribution). With the base Milky Way (MW) and UFD capture rates denoted as  $F_0^{\text{MW}}$  and  $F_0^{\text{UFD}}$ , one obtains [49] the full PBH-NS capture rates  $F = (\Omega_{\text{PBH}}/\Omega_{\text{DM}})F_0^{\text{MW}}$  and  $F = (\Omega_{\text{PBH}}/\Omega_{\text{DM}})F_0^{\text{UFD}}$  in the MW and UFD, respectively. The number of PBHs captured by a NS is  $Ft$ , where the time  $t$  is either  $t_G$  or  $t_{\text{UFD}}$  for the MW or the UFD, respectively. For our analysis we consider a typical NS with mass  $M_{\text{NS}} = 1.5 M_\odot$  and radius  $R_{\text{NS}} = 10 \text{ km}$ . The base NS-PBH capture rate  $F_0$  is given by [49]

$$F_0 = \sqrt{6\pi} \frac{\rho_{\text{DM}}}{m_{\text{PBH}}} \left( \frac{R_{\text{NS}} R_S}{\bar{v}(1 - R_S/R_{\text{NS}})} \right) (1 - e^{-3E_{\text{loss}}/(m_{\text{PBH}}\bar{v}^2)}), \quad (1)$$

where  $\bar{v}$  is the DM velocity dispersion, and  $R_S = 2GM_{\text{NS}}$  and  $R_{\text{NS}}$  are the BH Schwarzschild radius and the NS radius, respectively.  $E_{\text{loss}}$  is the energy loss associated with the PBH-NS interaction. BH capture can occur when  $E_{\text{loss}} > m_{\text{PBH}}v_0^2/2$ , with  $v_0$  being the asymptotic velocity of the PBH. Taking a uniform flux of PBHs across the star, the average energy loss for a typical NS is found to be  $E_{\text{loss}} \approx 58.8G^2m_{\text{PBH}}^2M_{\text{NS}}/R_{\text{NS}}^2$ . Since MSPs originate from

binaries, a higher binary gravitational potential causes an increase in the capture rate. We, therefore, assume that the capture rate for MSPs is a factor of 2 higher than for isolated NSs. For example, for typical values of parameters and  $m_{\text{PBH}} = 10^{19}$  g, one obtains

$$\begin{aligned} F_0^{\text{MW}} &= 1.5 \times 10^{-11} / \text{yr} \\ F_0^{\text{UFD}} &= 6.0 \times 10^{-10} / \text{yr}. \end{aligned} \quad (2)$$

For the MW we have used velocity dispersions of 48 km/s and 105 km/s for the NS and DM, respectively, as well as DM density  $8.8 \times 10^2 \text{ GeV/cm}^3$ . The pulsar and DM velocity dispersions are simultaneously taken into account for the MW as described below. For UFD we have used the DM velocity dispersion 2.5 km/s and the DM density  $10 \text{ GeV/cm}^3$ .

A PBH could also be captured by a NS progenitor prior to supernova core collapse [50], but this does not increase the capture rates significantly.

Natal pulsar kicks can enable pulsars to escape from the region of interest. We include this effect in our calculations (see Supplemental Material [51]).

Pulsar lifetimes in the presence of PBHs with a given number density can be estimated as  $\langle t_{\text{NS}} \rangle = 1/F + t_{\text{loss}} + t_{\text{con}}$ , where the first term describes the mean BH capture time,  $t_{\text{loss}}$  is the time for the PBH to be brought within the NS once it is gravitationally captured, and  $t_{\text{con}}$  is the time for the black hole to consume the NS. For a typical NS one finds [49] that  $t_{\text{loss}} \approx 4.1 \times 10^4 (m_{\text{PBH}}/10^{22} \text{ g})^{-3/2} \text{ yr}$ . The spherical accretion rate of NS matter onto the PBH is described by the Bondi equation  $dm_{\text{BH}}/dt = 4\pi\lambda_s G^2 m_{\text{BH}}^2 \rho_c / v_s^3 = C_0 m_{\text{BH}}^2$ , where  $m_{\text{BH}}(t)$  is the time-dependent mass of the central black hole,  $v_s$  is the sound speed,  $\rho_c$  is the central density, and  $\lambda_s$  is a density profile parameter. For typical NS values of [52]  $v_s = 0.17$ ,  $\rho_c = 10^{15} \text{ g/cm}^3$ , and  $\lambda_s = 0.707$  (for a star described by an  $n = 3$  polytrope) we obtain that  $t_{\text{con}} = 10(10^{19} \text{ g}/m_{\text{PBH}}) \text{ yr}$ . If PBHs make up all of the DM, we calculate that  $\langle t_{\text{NS}} \rangle < 10^{12} \text{ yr}$  for  $10^{17} \text{ g} < m_{\text{PBH}} < 10^{25} \text{ g}$ , implying that a  $\mathcal{O}(1-10)\%$  fraction of pulsars should have been consumed in the age of the Galaxy. This is consistent with observations [23] suggesting an underabundance of MSPs near the central Galactic black hole, Sgr A\*. A recently discovered young,  $4 \times 10^4$ -yr-old, magnetar J1745-2900 located just 0.1 pc from the GC [25,26] is also consistent with our results, since this magnetar's age is shorter than  $\langle t_{\text{NS}} \rangle$ . The unusual surface temperature [61] and x-ray luminosity of J1745-2900 warrants scrutiny, as this activity might be consistent with PBH destruction in progress.

Angular momentum transfer determines the dynamics of a NS spin-up. As the captured PBH starts to grow and consume the spinning pulsar from the inside, the radius of the neutron star decreases and angular momentum conservation forces a spin-up. As the star contracts, the

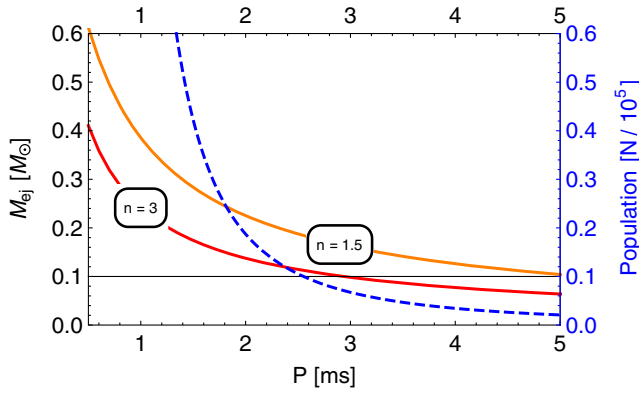


FIG. 1. Total ejected mass ( $M_{\text{ej}}$ ) from a MSP with initial rotation period  $P$  disrupted by a PBH.  $n = 3$  polytrope (red) and  $n = 1.5$  polytrope (orange) NS density profiles are shown. The black line indicates ejection of  $0.1 M_{\odot}$ . The MSP period-population distribution [47] is displayed with a dashed blue line.

fractional change in radius is greater for accreted matter in the inner regions than it is for material further out. This could lead to differential rotation. However, if angular momentum can be efficiently transferred outward, the star can maintain rigid-body rotation. Viscosity [53,54] and magnetic stresses [54] can prevent differential rotation from developing. It can be shown (see Supplemental Material [51]) that angular momentum is transferred efficiently on the relevant time scales and that Bondi accretion proceeds nearly uninterrupted throughout the BH evolution.

Ejected mass originates from the star spin-up when matter at the equator exceeds the escape velocity. Using polytropic NS density runs with different indices [52], we have calculated analytically the amount of ejected material (see the end of the Ejected Mass section in the Supplemental Material [51]). The results are shown in Fig. 1 for NS victims with a range of initial rotation periods. Based on our estimates discussed in Supplemental Material [51], NS with periods of a few ms can eject more than  $10^{-1} M_{\odot}$  of material. A detailed calculation taking into account general relativistic effects [62,63] is needed to improve understanding of the ejected mass.

The number of MSPs in the disk with periods greater than  $P$  is described by a power-law distributed population model [47]. We assume that the distribution in the CMZ is the same, and we normalize the total to the number of neutron stars produced in supernova explosions. According to the population model [47],  $N_{\text{MSP}} \approx 1.6 \times 10^4 (1.56 \text{ ms}/P)$ . Using the differential distribution  $d(N_{\text{MSP}})/dP$ , we obtain the population-averaged ejected mass:

$$\langle M_{\text{ej}} \rangle = \frac{\int_{P_{\text{min}}}^{\infty} \left( \frac{dN_{\text{MSP}}}{dP} \right) M_{\text{ej}}(P) dP}{\int_{P_{\text{min}}}^{\infty} \left( \frac{dN_{\text{MSP}}}{dP} \right) dP}, \quad (3)$$

where  $P_{\text{min}}$  is the minimal MSP period in the population, and  $M_{\text{ej}}(P)$  is the ejected mass function interpolated from the distribution shown in Fig. 1. We find that the

population-averaged ejected mass is  $\langle M_{\text{ej}} \rangle = 0.18 M_{\odot}$  and  $0.1 M_{\odot}$  if we take the shortest period to be  $P_{\text{min}} = 0.7 \text{ ms}$  (theoretically predicted) and  $P_{\text{min}} = 1.56 \text{ ms}$  (observed), respectively. Since realistic nuclear matter equations of state suggest flatter NS density profiles than our polytropic approximations, our estimate is conservative and  $\langle M_{\text{ej}} \rangle$  can be larger by up to a factor of a few. Alternative population models [46], such as those based on [48], do not significantly alter the results.

Nucleosynthesis takes place in the ejecta. Heating accompanying the growth of a BH inside a NS results in a temperature increase near the event horizon that is only a factor of a few higher than the NS surface temperature [53]:  $T_h/T_{\text{surf}} \sim 3$ . Consequently, neutrino emission is negligible and ejected material does not suffer significant heating or exposure to neutrinos.

Decompression of the centrifugally ejected, relatively low-entropy, and very-low-electron-fraction nuclear matter in this scenario could be expected to result in a significant mass fraction of this material participating in  $r$ -process nucleosynthesis [64–70]. The large neutron excess in this scenario, relatively unmolested by neutrino charged-current capture-induced reprocessing of the neutron-to-proton ratio, could lead to fission cycling [70,71], thereby tying together the nuclear mass number  $A = 130$  and  $A = 195$   $r$ -process abundance peaks. Unlike COM  $r$ -process ejecta, which will have a wide range of neutrino exposures, entropy, and electron fraction, and thereby can reproduce the solar system  $r$ -process abundance pattern [72], the PBH scenario may be challenged in producing the low-mass,  $A < 100$ ,  $r$ -process material.

The material ejected in the PBH-NS destruction process is heated by beta decay and fission, resulting in thermodynamic conditions and abundances closely akin to those in the COM-induced “tidal tail” nuclear matter decompression that gives rise to kilonovae-like electromagnetic signatures [34–41]. This could be a more-luminous and longer-duration transient compared to the classic COM-generated kilonovae, as the ejecta in the PBH scenario can have more mass than the tidal tails of COM.

The total amount of ejected  $r$ -process material in the PBH-NS destruction process can be estimated via  $M_{\text{tot}}^r = F t N_{\text{MSP}} \langle M_{\text{ej}} \rangle$ , assuming that the bulk of the ejecta undergoes  $r$ -process nucleosynthesis. The overall mass of  $r$ -process material in the Galaxy is  $M_{\text{tot}}^{r,\text{MW}} \sim 10^4 M_{\odot}$ . The required fraction of dark matter in the form of PBHs is  $(\Omega_{\text{PBH}}/\Omega_{\text{DM}}) = M_{\text{tot}}^{r,\text{MW}} / (F_0^{\text{MW}} t_G N_{\text{MSP}}^{\text{GC}} \langle M_{\text{ej}} \rangle)$ . If the mass of ejected  $r$ -process material in a single event is  $0.1 M_{\odot} - 0.5 M_{\odot}$ , the PBH capture rate  $10^{-5} - 10^{-6} \text{ Mpc}^{-3} \text{ yr}^{-1}$  can account for all of the  $r$ -process material in the Galaxy. At this rate,  $10^5$  NS disruption events have occurred in the lifetime of the Galaxy.

This rate of NS disruptions in UFDs is also consistent with the observationally inferred UFD  $r$ -process content

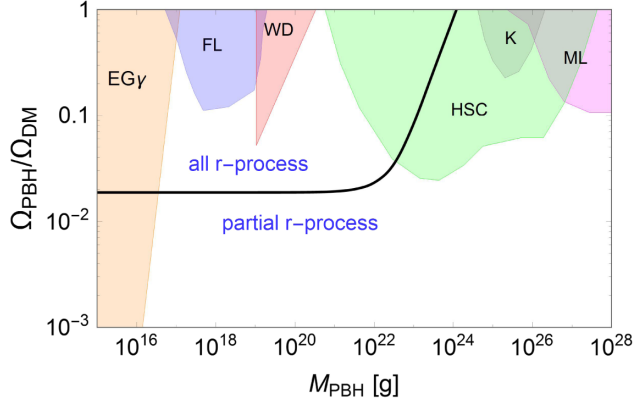


FIG. 2. Parameter space where PBHs can account for all or partial  $r$ -process element production in the Milky Way and the UFDs simultaneously. Constraints from extragalactic  $\gamma$ -rays from BH evaporation [74] (EG $\gamma$ ), femtolensing [75] (FL), white dwarf abundance [76] (WD), Kepler star milli- or microlensing [77] (K), Subaru HSC microlensing [78] (HSC), and MACHO, EROS, and OGLE microlensing [79] (ML) are displayed.

and with the uneven distribution of this material among the observed UFD. Observations imply that 1 in 10 UFDs have been a host to  $r$ -process nucleosynthesis events, which must, therefore, be rare [21,22,73]. The rate  $F_0^{\text{UFD}}$  implies that the probability of a NS disruption in a single UFD is about 0.1, which explains the uneven distribution. The amount of  $r$ -process material supplied by a single event,  $\sim 0.1 M_\odot$ , is more than sufficient to explain the observations [21,22,73]. Only a small fraction  $\sim (\bar{v}^{\text{UFD}}/v_\infty) \sim 10^{-3}$  of the produced  $r$ -process material is likely to remain in the shallow gravitational potential well of a UFD because it is produced with a velocity  $v_\infty \sim 0.1 v_{\text{esc}}$ . The observations are consistent with this: the required  $10^{-4} M_\odot$  of  $r$ -process material is consistent with a 0.1% fraction of the  $0.1 M_\odot$  produced in a single event.

We have separately fit to the  $r$ -process abundances for the MW and UFD, accounting for uncertainties in various quantities as described below. The combined requirements result in the allowed region of parameter space shown on Fig. 2, along with the current constraints for PBH contribution to the DM abundance. The region denoted “all  $r$ -process” shows parameter space for which  $r$ -process observations are fully explained simultaneously in the MW and in UFDs. For our fit we have varied the input parameters over a broad range, covering significant parameter space (see Supplemental Material [51]). The enclosed region above the line can be interpreted as a constraint on  $r$ -process material overproduction from PBH-NS interactions, subject to large uncertainties in astrophysical input parameters. Energy losses and capture rates for black holes with masses below  $\sim 10^{18}$  g are not well understood, and there is an uncertainty in the range of parameters for small masses.

We note that COM-produced  $r$  process, with an event rate of  $10^{-4}$ – $10^{-5}$  Mpc $^{-3}$  yr $^{-1}$ , could also be consistent with this

analysis [80]. However, COM simulations suggest an ejecta mass of  $\sim 0.01 M_\odot$ . This would imply a COM rate near the upper end of the allowed range, if COMs are to explain all of the  $r$ -process. Such a rate is still marginally consistent with the current Advanced LIGO (aLIGO) limits, but will be readily verifiable or refutable when aLIGO reaches its design sensitivity [81] in a few years. Sensitivity similar to aLIGO is expected in the upcoming Advanced Virgo [82] (aVirgo) and KAGRA [83] experiments. A recent analysis of kilonovae [84] also exhibits tension with observations and highlights the need for an extremely efficient ejection of  $r$ -process material in the COM scenario.

Positron emission from ejecta can explain the observed 511-keV emission line from the Galactic central region [85], which is consistent with the  $e^+e^-$  annihilation line via positronium formation. The origin of the positrons remains unknown [29]. The 511-keV line flux in the bulge component is  $\sim 10^{-3}$  photons cm $^{-2}$ s $^{-1}$  [86]. The line can be explained through electron-positron annihilations that occur at a rate of  $\Gamma(e^+e^- \rightarrow \gamma\gamma) \sim 10^{50}$  yr $^{-1}$ . Ejected cold nuclear matter expands on a dynamical time scale of  $\tau_e \sim \alpha/\sqrt{G_N \rho} = 446\alpha(\rho/\text{g cm}^{-3})^{-1/2}$ s, where  $\alpha = 0.01$ – $10$  is a model-dependent parameter [64,65,80]. At the same time, beta decays and fission raise the temperature to  $T \sim 0.1$  MeV [64,65,80]. This temperature is high enough to generate a sizable equilibrium density of positrons, which leak through the surface of each clump. Taking the radius of each clump as  $R \sim 0.1$  km and the density as  $\rho \sim 10^8$  g/cm $^3$ , the total surface area of  $0.1 M_\odot$  of ejected material is  $A \sim 4\pi R^2(0.1 M_\odot/\rho)/(4\pi R^3/3) \sim 10^{20}$  cm $^2$ . The number of positrons emitted in a single event, during the time  $\tau_e$ , while the temperature  $T \sim 0.1$  MeV is maintained, can be estimated as  $N_{e^+} \sim Av\tau_e \times 2(m_e T/2\pi)^{3/2} \exp(-m_e/T)$ , where  $v$  is the average speed of positrons emitted with a relativistic  $\gamma$  factor  $\gamma \sim (3T/m_e)$ . If the neutron star disruption events occur in the GC on the time scale of  $\tau_d \sim 10^5$  yr, the average rate of positron production is

$$R_{e^+} = N_{e^+}/\tau_d \sim 10^{50} \text{ yr}^{-1}. \quad (4)$$

Since the average positron energy  $E_{e^+} \approx 3T$  is below 3 MeV, the positrons do not annihilate in flight in the interstellar medium [87].

Fast radio bursts, kilonovae and other signatures are expected from the PBH capture-induced NS demise. During the final stages of the event, described by dynamical time scales of the order of a few to tens of milliseconds,  $10^{41}$ – $10^{43}$  ergs of energy stored in the magnetic field are released. Inside the cold NS, at temperatures below 0.4 MeV, the nuclear matter is a type-II superconductor and magnetic field is concentrated in flux tubes. A consequence of the rapid rearrangement of nuclear matter accompanying ejection is a prodigious release of electromagnetic radiation from magnetic field reconnection and decay. The resulting bursts of radio waves [31,32] with

duration of a few milliseconds can account for some of the observed [33] FRBs. One FRB is known to be a repeater, while the others appear to be one-time events. The FRB energy of  $10^{41}$  erg is consistent with observations [88]. If 1%–10% of the magnetic field energy is converted to radio waves, a FRB could accompany a NS destruction event. The rapidly evolving magnetic field can also accelerate charged particles leading to x-ray and  $\gamma$ -ray emission.

Detection of an “orphaned” kilonova (macronova) within the aLIGO, aVirgo, and KAGRA sensitivity distance ( $\sim 200$  Mpc) that is not accompanied by a binary compact object inspiral gravitational-wave signal or a short  $\gamma$ -ray burst, but possibly associated with a FRB, would constitute an indirect argument that NS disruptions via PBH capture occur and could account for a significant fraction of the  $r$  process. Sophisticated numerical simulations of PBH-induced NS collapse and of the accompanying nucleosynthesis and electromagnetic emission (including FRB) could help enable feasible observational search strategies. The search can be further assisted by detailed mapping of chemical abundances that will be made possible by the future Hitomi-2 detector. The stakes are high, as finding evidence for PBH-NS destruction could have profound implications for our understanding of the origin of the heavy elements and for the source and composition of dark matter.

We thank B. Carr, Y. Inoue, S. Nagataki, R. Rothschild, and E. Wright for helpful discussions. The work of G. M. F. was supported in part by National Science Foundation Grants No. PHY-1307372 and No. PHY-1614864. The work of A. K. and V. T. was supported by the U.S. Department of Energy Grant No. DE-SC0009937. A. K. was also supported by the World Premier International Research Center Initiative (WPI), MEXT, Japan.

\*gfuller@ucsd.edu

†kusenko@ucla.edu

‡vtakhist@physics.ucla.edu

[1] Y. B. Zel’dovich and I. D. Novikov, *Astronomicheskii Zhurnal* **43**, 758 (1966) [*Sov. Astron.* **10**, 602 (1967)].  
 [2] S. Hawking, *Mon. Not. R. Astron. Soc.* **152**, 75 (1971).  
 [3] B. J. Carr and S. W. Hawking, *Mon. Not. R. Astron. Soc.* **168**, 399 (1974).  
 [4] J. Garcia-Bellido, A. D. Linde, and D. Wands, *Phys. Rev. D* **54**, 6040 (1996).  
 [5] M. Yu. Khlopov, *Res. Astron. Astrophys.* **10**, 495 (2010).  
 [6] P. H. Frampton, M. Kawasaki, F. Takahashi, and T. T. Yanagida, *J. Cosmol. Astropart. Phys.* **04** (2010) 023.  
 [7] M. Kawasaki, A. Kusenko, and T. T. Yanagida, *Phys. Lett. B* **711**, 1 (2012).  
 [8] M. Kawasaki, A. Kusenko, Y. Tada, and T. T. Yanagida, *Phys. Rev. D* **94**, 083523 (2016).  
 [9] E. Cotner and A. Kusenko, *arXiv:1612.02529*.  
 [10] B. Carr, F. Kuhnel, and M. Sandstad, *Phys. Rev. D* **94**, 083504 (2016).

[11] K. Inomata, M. Kawasaki, K. Mukaida, Y. Tada, and T. T. Yanagida, *Phys. Rev. D* **95**, 123510 (2017).  
 [12] K. Inomata, M. Kawasaki, K. Mukaida, Y. Tada, and T. T. Yanagida, *arXiv:1701.02544*.  
 [13] J. Georg and S. Watson, *arXiv:1703.04825*.  
 [14] M. E. Burbidge, G. R. Burbidge, W. A. Fowler, and F. Hoyle, *Rev. Mod. Phys.* **29**, 547 (1957).  
 [15] M. Arnould, S. Goriely, and K. Takahashi, *Phys. Rep.* **450**, 97 (2007).  
 [16] A. G. W. Cameron, *Publ. Astron. Soc. Pac.* **69**, 201 (1957).  
 [17] J. W. Truran, J. J. Cowan, C. A. Pilachowski, and C. Sneden, *Publ. Astron. Soc. Pac.* **114**, 1293 (2002).  
 [18] Y. Z. Qian and G. J. Wasserburg, *Phys. Rep.* **442**, 237 (2007).  
 [19] D. Argast, M. Samland, F. K. Thielemann, and Y. Z. Qian, *Astron. Astrophys.* **416**, 997 (2004).  
 [20] C. Freiburghaus, S. Rosswog, and F.-K. Thielemann, *Astrophys. J. Lett.* **525**, L121 (1999).  
 [21] A. P. Ji, A. Frebel, A. Chiti, and J. D. Simon, *Nature (London)* **531**, 610 (2016).  
 [22] P. Beniamini, K. Hotokezaka, and T. Piran, *Astrophys. J.* **832**, 149 (2016).  
 [23] J. Dexter and R. M. O’Leary, *Astrophys. J.* **783**, L7 (2014).  
 [24] J. Bramante and T. Linden, *Astrophys. J.* **826**, 57 (2016).  
 [25] K. Mori *et al.*, *Astrophys. J.* **770**, L23 (2013).  
 [26] J. A. Kennea *et al.*, *Astrophys. J.* **770**, L24 (2013).  
 [27] J. D. Bradford, M. Geha, R. R. Muñoz, F. A. Santana, J. D. Simon, P. Côté, P. B. Stetson, E. Kirby, and S. G. Djorgovski, *Astrophys. J.* **743**, 167 (2011); **778**, 85(E) (2013).  
 [28] R. Ibata, C. Nipoti, A. Sollima, M. Bellazzini, S. C. Chapman, and E. Dalessandro, *Mon. Not. R. Astron. Soc.* **428**, 3648 (2013).  
 [29] N. Prantzos *et al.*, *Rev. Mod. Phys.* **83**, 1001 (2011).  
 [30] R. E. Lingenfelter, J. C. Higdon, and R. E. Rothschild, *Phys. Rev. Lett.* **103**, 031301 (2009).  
 [31] J. Fuller and C. Ott, *Mon. Not. R. Astron. Soc.* **450**, L71 (2015).  
 [32] Z. Shand, A. Ouyed, N. Koning, and R. Ouyed, *Res. Astron. Astrophys.* **16**, 080 (2016).  
 [33] D. R. Lorimer, M. Bailes, M. A. McLaughlin, D. J. Narkevic, and F. Crawford, *Science* **318**, 777 (2007).  
 [34] D. Kasen, R. Fernandez, and B. Metzger, *Mon. Not. R. Astron. Soc.* **450**, 1777 (2015).  
 [35] L.-X. Li and B. Paczynski, *Astrophys. J.* **507**, L59 (1998).  
 [36] B. D. Metzger, G. Martínez-Pinedo, S. Darbha, E. Quataert, A. Arcones, D. Kasen, R. Thomas, P. Nugent, I. V. Panov, and N. T. Zinner, *Mon. Not. R. Astron. Soc.* **406**, 2650 (2010).  
 [37] L. F. Roberts, D. Kasen, W. H. Lee, and E. Ramirez-Ruiz, *Astrophys. J.* **736**, L21 (2011).  
 [38] K. Hotokezaka and T. Piran, *Mon. Not. R. Astron. Soc.* **450**, 1430 (2015).  
 [39] T. Piran, E. Nakar, and S. Rosswog, *Mon. Not. R. Astron. Soc.* **430**, 2121 (2013).  
 [40] J. Barnes and D. Kasen, *Astrophys. J.* **775**, 18 (2013).  
 [41] D. Martin, A. Perego, A. Arcones, F.-K. Thielemann, O. Korobkin, and S. Rosswog, *Astrophys. J.* **813**, 2 (2015).  
 [42] J. I. Read, L. Mayer, A. M. Brooks, F. Governato, and G. Lake, *Mon. Not. R. Astron. Soc.* **397**, 44 (2009).  
 [43] J. I. Read, G. Lake, O. Agertz, and V. P. Debattista, *Mon. Not. R. Astron. Soc.* **389**, 1041 (2008).

- [44] R. M. O’Leary, M. D. Kistler, M. Kerr, and J. Dexter, [arXiv:1601.05797](https://arxiv.org/abs/1601.05797).
- [45] M. Ajello *et al.* (Fermi-LAT Collaboration), *Astrophys. J.* **819**, 44 (2016).
- [46] D. R. Lorimer, *IAU Symp.* **291**, 237 (2013).
- [47] J. M. Cordes and D. F. Chernoff, *Astrophys. J.* **482**, 971 (1997).
- [48] C.-A. Faucher-Giguere and V. M. Kaspi, *Astrophys. J.* **643**, 332 (2006).
- [49] F. Capela, M. Pshirkov, and P. Tinyakov, *Phys. Rev. D* **87**, 123524 (2013).
- [50] F. Capela, M. Pshirkov, and P. Tinyakov, *Phys. Rev. D* **90**, 083507 (2014).
- [51] See Supplemental Material at <http://link.aps.org/supplemental/10.1103/PhysRevLett.119.061101>, which includes Refs. [24,42,43,47,52–60], for further details regarding pulsar kicks, viscosity, and magnetic differential rotation breaking, angular momentum transfer, as well as variation of various input parameters for the fit.
- [52] S. L. Shapiro and S. A. Teukolsky, *Black Holes, White Dwarfs, and Neutron Stars* (Wiley-Interscience, New York, 1983), pp. 1–663.
- [53] C. Kouvaris and P. Tinyakov, *Phys. Rev. D* **90**, 043512 (2014).
- [54] D. Markovic, *Mon. Not. R. Astron. Soc.* **277**, 25 (1995).
- [55] S. L. Shapiro and M. Shibata, *Astrophys. J.* **577**, 904 (2002).
- [56] M. Kaplinghat, R. E. Keeley, T. Linden, and H.-B. Yu, *Phys. Rev. Lett.* **113**, 021302 (2014).
- [57] J. F. Navarro, C. S. Frenk, and S. D. M. White, *Astrophys. J.* **490**, 493 (1997).
- [58] S. E. Kopusov *et al.*, *Astrophys. J.* **811**, 62 (2015).
- [59] A. Burkert, *IAU Symp.* **171**, 175 (1996); *Astrophys. J.* **447**, L25 (1995).
- [60] A. G. Lyne, R. N. Manchester, D. R. Lorimer, M. Bailes, N. D’Amico, T. M. Tauris, S. Johnston, J. F. Bell, and L. Nicastro, *Mon. Not. R. Astron. Soc.* **295**, 743 (1998).
- [61] F. C. Zelati *et al.*, *Mon. Not. R. Astron. Soc.* **449**, 2685 (2015).
- [62] N. Andersson and K. D. Kokkotas, *Int. J. Mod. Phys. D* **10**, 381 (2001).
- [63] B. J. Owen, L. Lindblom, C. Cutler, B. F. Schutz, A. Vecchio, and N. Andersson, *Phys. Rev. D* **58**, 084020 (1998).
- [64] J. M. Lattimer, F. Mackie, D. G. Ravenhall, and D. N. Schramm, *Astrophys. J.* **213**, 225 (1977).
- [65] B. S. Meyer, *Astrophys. J.* **343**, 254 (1989).
- [66] J. Lippuner and L. F. Roberts, *Astrophys. J.* **815**, 82 (2015).
- [67] P. Jaikumar, B. S. Meyer, K. Otsuki, and R. Ouyed, *Astron. Astrophys.* **471**, 227 (2007).
- [68] S. Goriely, A. Bauswein, and H. T. Janka, *Astrophys. J.* **738**, L32 (2011).
- [69] S. Goriely, A. Bauswein, H.-T. Janka, S. Panebianco, J.-L. Sida, J.-F. Lemaître, S. Hilaire, and N. Dubray, *J. Phys. Conf. Ser.* **665**, 012052 (2016).
- [70] M. Eichler *et al.*, *Astrophys. J.* **808**, 30 (2015).
- [71] M. R. Mumpower, G. C. McLaughlin, R. Surman, and A. W. Steiner, *Astrophys. J.* **833**, 282 (2016).
- [72] S. Wanajo, Y. Sekiguchi, N. Nishimura, K. Kiuchi, K. Kyutoku, and M. Shibata, *Astrophys. J.* **789**, L39 (2014).
- [73] Y. Hirai, Y. Ishimaru, T. R. Saitoh, M. S. Fujii, J. Hidaka, and T. Kajino, *Astrophys. J.* **814**, 41 (2015).
- [74] B. J. Carr, K. Kohri, Y. Sendouda, and J. Yokoyama, *Phys. Rev. D* **81**, 104019 (2010).
- [75] A. Barnacka, J. F. Glicenstein, and R. Moderski, *Phys. Rev. D* **86**, 043001 (2012).
- [76] P. W. Graham, S. Rajendran, and J. Varela, *Phys. Rev. D* **92**, 063007 (2015).
- [77] K. Griest, A. M. Cieplak, and M. J. Lehner, *Astrophys. J.* **786**, 158 (2014).
- [78] H. Niikura *et al.*, [arXiv:1701.02151](https://arxiv.org/abs/1701.02151).
- [79] P. Tisserand *et al.* (EROS-2 Collaboration), *Astron. Astrophys.* **469**, 387 (2007).
- [80] S. Goriely, N. Chamel, H. T. Janka, and J. M. Pearson, *Astron. Astrophys.* **531**, A78 (2011).
- [81] B. Cote, K. Belczynski, C. L. Fryer, C. Ritter, A. Paul, B. Wehmeyer, and B. W. O’Shea, *Astrophys. J.* **836**, 230 (2017).
- [82] F. Acernese *et al.* (VIRGO Collaboration), *Classical Quantum Gravity* **32**, 024001 (2015).
- [83] Y. Aso, Y. Michimura, K. Somiya, M. Ando, O. Miyakawa, T. Sekiguchi, D. Tatsumi, and H. Yamamoto (KAGRA Collaboration), *Phys. Rev. D* **88**, 043007 (2013).
- [84] Z.-P. Jin, K. Hotokezaka, X. Li, M. Tanaka, P. D’Avanzo, Y.-Z. Fan, S. Covino, D.-M. Wei, and T. Piran, *Nat. Commun.* **7**, 12898 (2016).
- [85] P. Jean *et al.*, *Astron. Astrophys.* **407**, L55 (2003).
- [86] J. Knodlseder *et al.*, *Astron. Astrophys.* **411**, L457 (2003).
- [87] J. F. Beacom and H. Yuksel, *Phys. Rev. Lett.* **97**, 071102 (2006).
- [88] K. Dolag, B. M. Gaensler, A. M. Beck, and M. C. Beck, *Mon. Not. R. Astron. Soc.* **451**, 4277 (2015).